Proteomic analysis of differential anther development from sterile/fertile lines in *Capsicum annuum* L.

Hongxia Pei [1, 2], **Hua Xie** [2], **Xuemei Wang** [2], **Xiujuan Yan** [2], **Baike Wang** [3], **Haiping Feng** [2], **Yunxia Zhao** [2], **Jingxia Gao** [Corresp., 2], **Jie Gao** [Corresp. 1]

[1] College of Forestry and Horticulture, Xinjiang Agricultural University, Urumqi 830052, China

[2] Institute of Horticulture Crops, Ningxia Academy of Agriculture and Forestry Sciences, Yinchuan 750002, China

[3] Institute of Horticulture Crops, Xinjiang Academy of Agricultural Sciences, Urumqi 830091, China

Corresponding Authors: Jingxia Gao, Jie Gao
Email address: gjj830114@163.com, ofc111@163.com

Background: Pepper (*Capsicum annuum* L.) is a major cash crop throughout the world. Male sterility is an important characteristic in crop species that leads to a failure to produce functional pollen, and it has crucial roles in agricultural breeding and the utilization of heterosis. **Objectives:** In this study, we identified many crucial factors and important components in metabolic pathways in anther and pollen development, and elucidated the molecular mechanism related to pollen abortion in pepper. **Methods:** Pepper pollen was observed at different stages to detect the characteristics associated with male sterility and fertility. The phytohormone and oxidoreductase activities were detected in spectrophotometric and redox reaction assays, respectively. Proteins were extracted from male sterile and fertile pepper lines, and identified by TMT/iTRAQ (Tandem mass tags/isobaric tags for relative and absolute quantitation) and LC-MS/MS (liquid chromatograph-mass spectrometer) analysis. Differentially abundant proteins (DAPs) were analyzed based on Gene Ontology annotations and the Kyoto Encyclopedia of Genes and Genomes database according to |fold change)| > 1.3 and *P* value < 0.05. DAPs were quantified in the meiosis, tetrad, and binucleate stages by parallel reaction monitoring (PRM).**Results:** In this study, we screened and identified one male sterile pepper line with abnormal cytological characteristics in terms of pollen development. The peroxidase and catalase enzyme activities were significantly reduced and increased, respectively, in the male sterile line compared with the male fertile line. Phytohormone analysis demonstrated that the gibberellin, jasmonic acid, and auxin contents changed by different extents in the male sterile pepper line. Proteome analysis screened 1645 DAPs in six clusters, which were mainly associated with the chloroplast and cytoplasm based on their similar expression levels. According to proteome analysis, 45 DAPs were quantitatively identified in the meiosis, tetrad, and binucleate stages by PRM, which were related to monoterpenoid

biosynthesis, and starch and sucrose metabolism pathways. **Conclusions:** We screened 1645 DAPs by proteomic analysis and 45 DAPs were related to anther and pollen development in a male sterile pepper line. In addition, the activities of peroxidase and catalase as well as the abundances of phytohormones such as gibberellin, jasmonic acid, and auxin were related to male sterility. The results obtained in this study provide insights into the molecular mechanism responsible for male sterility and fertility in pepper.

1   **Proteomic analysis of differential anther development in sterile/fertile lines**

2   **of *Capsicum annuum* L.**

4   Hongxia Pei[1,2], Hua Xie[2], Xuemei Wang[2], Xiujuan Yan[2], Baike Wang[3], Haiping Feng[2],

5   Yunxia Zhao[2], Jingxia Gao[2,*], Jie Gao[1,*]

7   [1] College of Forestry and Horticulture, Xinjiang Agricultural University, Urumqi 830052,

8   China

9   [2] Institute of Horticulture Crops, Ningxia Academy of Agriculture and Forestry Sciences,

10   Yinchuan 750002, China

11   [3] Institute of Horticulture Crops, Xinjiang Academy of Agricultural Sciences, Urumqi 830091,

12   China

13   * These authors contributed equally to this work.

14   **Corresponding Author:**

15   Jie Gao, College of Forestry and Horticulture, Xinjiang Agricultural University, Urumqi

16   830052, China;

17   Jingxia Gao, Institute of Horticulture Crops, Ningxia Academy of Agriculture and Forestry

18   Sciences, Yinchuan 750002, China

19   **Email address:** Jingxia Gao, E-mail: gjj830114@163.com

20   Jie Gao, Email: ofc111@163.com

Abstract

Background: Pepper (*Capsicum annuum* L.) is a major cash crop throughout the world. Male sterility is an important characteristic in crop species that leads to a failure to produce functional pollen, and it has crucial roles in agricultural breeding and the utilization of heterosis.

Objectives: In this study, we identified many crucial factors and important components in metabolic pathways in anther and pollen development, and elucidated the molecular mechanism related to pollen abortion in pepper.

Methods: Pepper pollen was observed at different stages to detect the characteristics associated with male sterility and fertility. The phytohormone and oxidoreductase activities were detected in spectrophotometric and redox reaction assays, respectively. Proteins were extracted from male sterile and fertile pepper lines, and identified by TMT/iTRAQ (Tandem mass tags/isobaric tags for relative and absolute quantitation) and LC-MS/MS (liquid chromatograph-mass spectrometer) analysis. Differentially abundant proteins (DAPs) were analyzed based on Gene Ontology annotations and the Kyoto Encyclopedia of Genes and Genomes database according to |fold change)| > 1.3 and *P* value < 0.05. DAPs were quantified in the meiosis, tetrad, and binucleate

42   stages by parallel reaction monitoring (PRM).

43   **Results:** In this study, we screened and identified one male sterile pepper line with abnormal

44   cytological characteristics in terms of pollen development. The peroxidase and catalase enzyme

45   activities were significantly reduced and increased, respectively, in the male sterile line

46   compared with the male fertile line. Phytohormone analysis demonstrated that the gibberellin,

47   jasmonic acid, and auxin contents changed by different extents in the male sterile pepper line.

48   Proteome analysis screened 1645 DAPs in six clusters, which were mainly associated with the

49   chloroplast and cytoplasm based on their similar expression levels. According to proteome

50   analysis, 45 DAPs were quantitatively identified in the meiosis, tetrad, and binucleate stages by

51   PRM, which were related to monoterpenoid biosynthesis, and starch and sucrose metabolism

52   pathways.

53   **Conclusions:** We screened 1645 DAPs by proteomic analysis and 45 DAPs were related to

54   anther and pollen development in a male sterile pepper line. In addition, the activities of

55   peroxidase and catalase as well as the abundances of phytohormones such as gibberellin,

56   jasmonic acid, and auxin were related to male sterility. The results obtained in this study provide

57   insights into the molecular mechanism responsible for male sterility and fertility in pepper.

58

59   **Keywords**: Male sterility, proteomic, Parallel reaction monitoring (PRM), Phytohormone,

60   Pepper (*Capsicum annuum* L.)

61

62   **BACKGROUND**

63   Pepper is a crucial crop plant that is cultivated throughout the world. During pollen development

64   in flowering plants, the anther structure comprising non-reproductive and reproductive tissues is

65   enveloped by the tapetum, middle layer, endodermis, and epidermis layers from the interior to

66   the exterior surface of pollen (Ning et al. 2019; van der Linde & Walbot 2019). Among these

67   structures, the tapetum acts as a nutrient source during anther development. During anther

68   development, the microspores must acquire nutrients, sporopollenin precursors, and metabolites

69   from the tapetum, where the inner layer of the anther wall acts as a physiological bridge between

70   the microspores (Ariizumi & Toriyama 2011; Blackmore et al. 2007). The sporogenous cells are

71   surrounded by the pollen sac and they form many pollen mother cells, which then form the

72   microspore tetrad. Finally, microspores are released from the tapetum layer to form the mature

73   pollen grains (Ariizumi & Toriyama 2011; Blackmore et al. 2007). All of these development

74   processes are essential for pollen formation and development. A recent study showed that tapetal

75   cell development, degradation, and microspore development are closely related to male fertility

76   (Guo et al. 2018). Male sterility is characterized by abnormal male organ development and the

77   failure to produce normal pollen grains. Male sterility in plants can be divided into genetic male

78   sterility and cytoplasmic male sterility (Bohra et al. 2016). Cytoplasmic male sterility involves

79   the suppression of functional pollen grain development, which is controlled by mitochondrial

80   genes. By contrast, genetic male sterility is controlled by a pair of nuclear genes, which are

81   stably transferred to the offspring (Kim & Kim 2006; Yuan et al. 2018).

82   In genetic breeding, the male sterility system has been applied as an effective strategy to

83   achieve heterosis in flowering plants, such as rice, cotton, and wheat (Cheng et al. 2020;

84   Melonek et al. 2021; Tang et al. 2017). In a previous study, the rice fertility genes *OsNP1* and

85   *ZmAA1* were expressed in the nuclear sterile mutant osnp1-1 to ultimately create a genetically

86   stable sterile line (Zhen18A) and its maintainer line (Zhen18B) (Chang et al. 2016a). Recently, a

87   deficient male-sterile mutant constructed using the CRISPR/Cas9 technique was transformed

88   with a recombinant vector cassette containing *orfH79* and *CYP703A3* to obtain the maintainer

89   line 9311-3B for heterosis breeding (Song et al. 2021). Therefore, understanding and controlling

90   the molecular mechanisms responsible for male sterility are beneficial for plant breeders. Thus,

91   many previous studies have aimed to identify candidate genes related to the control of

92   cytoplasmic male sterility and the associated molecular mechanisms. For example, MutS

93   HOMOLOG1 (MSH1) affects fertility reversion from cytoplasmic male sterility in *Brassica*

94   *juncea* (Zhao et al. 2021b). The RFL24 protein in *Arabidopsis thaliana* is a mitochondrial-

95   targeted pentatricopeptide repeat that can inhibit mitochondrial genes related to male gametes to

96   cause cytoplasmic male sterility (Durand et al. 2021). A recent study found that Rf1 and Rf3

97   candidates in hybrid wheat can bind to the mitochondrial *orf279* transcript and induce its

98   cleavage to prevent the expression of cytoplasmic male sterility, thereby restoring normal pollen

99   production in transgenic wheat plants (Geyer et al. 2016; Melonek et al. 2021). The *atp6-2* gene

100   in pepper species encodes a subunit of the mitochondrial ATP synthase complex and it may be

101   responsible for the male sterility trait due to a deletion at the 3′-end of the male sterility allele

102   (Arimura et al. 2020; Kim & Kim 2006). A strong candidate gene for the male sterile, orf507,

103   harbors a single nucleotide misssing which leads the open reading frame shift to 507 bp(Gulyas

104   et al. 2010).

105   The increasing availability of male-sterile genomes and transcriptome sequences has

106   facilitated the identification of candidate factors related to cytoplasmic male sterility. In

107   particular, transcriptome analysis of pepper 8214A and 8214B anthers detected 1355

108   differentially expressed genes, including ubiquitin ligase genes, methyltransferase genes, and cell

109   cycle-related genes (Qiu et al. 2018). In addition, transcriptional analysis of flower buds from a

110   pepper sterile line and restorer line identified eight genes related to the phosphatidylinositol

111   signaling system, and inositol phosphate metabolism was associated with fertility restoration

112   (Wei et al. 2019). In pepper, 1069 differentially expressed genes and 764 differentially expressed

113   proteins were identified based on proteomic and transcriptomic sequences, respectively, and the

114   *TDF1* and *AMS* genes were associated with tapetum and pollen exine formation (Cheng et al.

115   2019). However, it is unclear how these candidate genes might influence male sterility.

116   Proteomics is a powerful high-throughput method for screening candidate proteins and

117   identifying molecular mechanisms related to male sterility pathways (Sheoran & Sawhney 2010;

118   Wen et al. 2007; Zhang et al. 2018). For example, 1390 differentially abundant proteins (DAPs)

119   associated with cytosolic ascorbate peroxidase, carbohydrate metabolism, gibberellin 20-oxidase,

120   and enolase were identified in the nuclear male-sterile cotton line ms5ms6 (Wang et al. 2019).

121   Thus, proteomics analysis is advantageous for exploring global protein expression and resolving

122   the molecular mechanisms related to pollen abortion and pollen development. However, in

123   pepper species, only a limited number of candidate proteins (23 distinct proteins) have been

124   screened and identified by two-dimensional gel electrophoresis (Wu et al. 2013), and thus little

125   proteomic information is available for exploring the mechanisms related to male sterility in

126   pepper species.

127   In this study, we screened and identified a male sterile pepper line based on the morphological

128   features of pollen. The peroxidase (POD) enzyme activity was significantly reduced in a male

129   sterile line compared with a fertile pepper line, whereas the catalase (CAT) enzyme activity was

130   significantly increased. Phytohormone analysis indicated that the gibberellin, jasmonic acid, and

131   auxin   contents differed in the male sterile pepper line compared with the fertile line.

132   Furthermore, 1645 DAPs were identified in the meiosis, tetrad, and binucleate stages using high-

133   throughput proteomics. These DAPs were mainly distributed in the chloroplast and cytoplasm. In

134   total, 45 DAPs were quantitatively identified in the meiosis, tetrad, and binucleate stages by

135   parallel reaction monitoring (PRM), and they were related to monoterpenoid biosynthesis, and

136   starch and sucrose metabolism pathways. Our results provide new insights into the important

137   proteins for male sterility and the associated molecular mechanisms, thereby facilitating the

138   cloning of genes related to male sterility.

139

140   **METHODS**

141   **Plant materials and growth conditions**

142   Male fertile and sterile pepper lines were grown in a greenhouse according to standard

143   agronomic practices. During flowering, flower buds were collected at different development

144   stages (meiosis, microspore tetrad, binucleate, and microspore stages) and cytological

145 observations were conducted using an Olympus CX31 microscope. In addition, three biological

146 replicates of fertile and sterile anthers were collected and frozen rapidly in liquid nitrogen, before

147 storing at −80°C for proteomic analysis.

148

Cytological observations

150 Flower buds were collected and fixed in formalin:acetic acid:alcohol (ethanol:acetic

151 acid:formaldehyde:double-distilled H_2O = 10:1:2:7) for 24 h at different development stages to

152 make cytological observations of semithin sections. The materials were then washed three times

153 with 200 μL of 0.2 M phosphate-buffered saline and dehydrated with an ethanol concentration

154 gradient. Finally, the samples were embedded in resin for 24 h and sectioned to obtain transverse

155 slices using a microtome. The transverse slices were stained with 1.5–2% toluidine blue (Liu et

156 al. 2014; Lou et al. 2007), before photographing using an Olympus CX31 microscope. In

157 addition, pollen grains were collected from anthers using tweezers to determine their viability.

158 The pollen grains were stained with aceto-carmine and photographed using an optical

159 microscope.

Detection of enzyme activities and plant hormone contents

161 Samples of flower buds at different stages were collected and ground in liquid nitrogen to

162 determine the oxidordeuctase enzyme activities. The ground powdered samples were extracted

163 and incubated in extraction buffer. The homogenate was centrifuged at 8000 × g and 4°C for 15

164 min, and the supernatant solution was used to determine the enzyme activities with extraction

165 kits according to the manufacturer's instructions.

166 To determine the plant hormone contents, the soluble supernatant was extracted from 0.1 g of

167 flower bud samples collected at different stages after homogenizing at 4°C overnight in 1 mL of

168 chilled buffer (methanol:double-distilled H_2O:acetic acid = 80:20:1). The residue was extracted

169 in chilled buffer after centrifugation at 8000 × g for 10 min. The residue was centrifuged and

170   heated up to 40°C under a stream of nitrogen. The sample was extracted and decolorized three

171   times in 0.5 mL of petroleum ether at 60–90°C. Saturated citric acid aqueous solution was then

172   added to the sample. Finally, the sample was spun to mix well after adding 0.5 mL of methanol

173   and used for spectrophotometric assays.

174

175   **Protein extraction, TMT labeling, HPLC (High Performance Liquid Chromatography)**

176   **fractionation, and LC-MS/MS analysis**

177   All samples for protein extraction were ground in liquid nitrogen and sonicated three times

178   using an ultrasonic processor in cool lysis buffer (8 M urea and 1% protease inhibitor). Each

179   solution was centrifuged at 12,000 × g and 4°C for 10 min. The protein concentration in the

180   supernatant was assayed using a BCA kit according to the manufacturer's instructions. To digest

181   the proteins, 5 mM dithiothreitol was added to the supernatant solution, which was heated for 30

182   min at 56°C and then treated with 10 mM iodoacetamide to alkylate for 15 min at 56°C in

183   darkness. The protein solution was diluted with 100 μL of 50 mM triethylammonium bicarbonate.

184   Finally, trypsin was added to the protein sample solution at a trypsin:protein mass ratio of 1:50

185   and the first protein digestion was conducted overnight at 37°C. For the second protein digestion,

186   the trypsin:protein mass ratio was 1:100.

187   For the TMT/iTRAQ assay, 0.5 M triethylammonium bicarbonate was added to the peptide

188   solution and reconstituted using the TMT/iTRAQ kit. One unit of reagent was thawed in

189   acetonitrile for 2 h at 25°C. All peptides were subjected to LC-MS/MS analysis using nano-flow

190   liquid chromatography tandem mass spectrometry (LC-MS) with an EASY-nLC 1200 UPLC

191   system connected to a Q Exactive™ Plus quadrupole orbitrap mass spectrometer.

192

193   **Protein identification and bioinformatics analysis**

194   For Protein identification, raw data were searched against *Capsicum_annuum_*4072 database

195   (35548 entries) concatenated with reverse decoy database by Proteome Discoverer search engine

196   (V2.4.1.15) . Two missing cleavages were allowed using Trypsin cleavage enzyme. The mass

197   tolerance for precursor ions was 10 ppm and fragment ions was 0.02 Da. Carbamidomethyl on

198   Cys, TMT-6plex (N-terminus) and TMT-6plex (K) were specified as fixed modifications. In

199   addition, oxidation on Met and acetylation (N-terminus) were as variable modifications.

200   Quantitative method was set as TMT-6plex. FDR was adjusted to 1% and minimum score for

201   modified peptides was set > 40. Minimum peptide length was set at 6. The raw data and results

202   were submitted on ProteomeXchange (accession:PXD031331).

203   For differentially expressed proteins analysis, firstly, the expression ratio of each protein

204   between two samples with multiple replicates were obtained and calculate the average value.

205   Then, the significance p value of differentially expressed proteins was calculated by the two-

206   tailed T-test method. DAPs with p value <0.05 and expression ratio > 1.3 were up-regulated,

207   while DAPs with p value <0.05 and expression ratio < 1/1.3 were down-regulated proteins.

208   All DAPs were functionally classified into biological processes, molecular functions, and

209   cellular components based on Gene Ontology (GO) annotations (http://www.geneontology.org/),

210   and enriched subcategories and metabolic pathways using the Kyoto Encyclopedia of Genes and

211   Genomes (KEGG) database (http://www.genome.jp/kegg/pathway.html). In addition, all DAPs

212   were searched against the STRING database (V10.1) to detect protein–protein interactions (PPIs)

213   based on confidence score > 0.7. *Arabidopsis thaliana* was used as the reference species for

214   establishing PPI networks. Data visualization in venn diagram were used by Tbtools software

215   (Chen et al., 2020). The PCA diagram, volcano plot and heat map were completed by online

216   software (ptmbiolab.com). The bar charts in this study were made by origin software (V.7.0).

217   **Targeted protein quantification by PRM**

218   Protein extraction and trypsin digestion were performed in the TMT experiment for targeted

219   protein quantification. After LC-MS/MS analysis, the data obtained for each sample were

220 processed using the PRM acquisition method to quantify the abundances of targeted proteins.

221 Each protein with more than two unique peptides was quantified, but only one peptide segment

222 was identified for some proteins due to sensitivity and other reasons. Three biological replicates

223 of each sample were performed and 15–20 proteins were randomly selected and quantified. PRM

224 analysis was conducted by Jingjie PTM BioLabs (Hangzhou, China) for this study.

225

226 **RESULTS**

227 **Differential anther development in male sterile and fertile pepper lines**

228 We screened one putative male sterile pepper line that produced few pollen grains compared

229 with the fertile pepper line. To confirm the pollen abortion characteristics in the male sterile

230 pepper line, we observed the morphological differences in anther development during different

231 stages using semi-thin sections. No obvious differences were found between the fertile and

232 sterile male lines in the sporogenous cell stage and the pollen mother cell stage (Figures 1A, 1B,

233 1H, and 1I). The nucleus volume was larger and the microspore mother cells entered meiosis in

234 the male sterile line (Figure 1C). Observations of tapetum cells indicated that they disintegrated

235 in the male sterile line (Figure 1J). Furthermore, the stained microspores were dispersed in the

236 chamber in the microspore stage in the fertile pepper line (Figure 1D–F). By contrast, the

237 microspores were crushed and disintegrated, and they adhered to the tapetum to form a dense

238 belt in the male sterile line (Figure 1K–M). In the last stage of pollen development, normal

239 grains were clearly observed during pollen maturation in the fertile pepper line (Figure 1G),

240 whereas a thin layer of tapetum cells formed a dense belt without mature pollen in the sterile line

241 (Figure 1N). Thus, morphological observations indicated that premature tapetum death may have

242 been the cause of male sterility.

243 To further assess the viability of the pollen grains, anthers were collected and the pollen grains

244 were stained with aceto-carmine. Interestingly, large amounts of the pollen grains were strongly

245   stained in the fertile pepper line (Figure 1O), whereas none of the pollen grains stained in the

246   male sterile line (Figure 1P). These results suggest that male sterility may have been due to the

247   production of few pollen grains and their infertility.

248

249   **Antioxidant enzyme activities in different anther development stages in male sterile and**

250   **fertile pepper lines**

251   We investigated the differences in the activities of antioxidant enzymes during anther

252   development in the male sterile (BY) and fertile (KY) pepper lines. In particular, the superoxide

253   dismutase (SOD), CAT, POD, and malondialdehyde enzyme activity levels were compared in

254   three anther development stages (microspore tetrad, meiosis, and uninucleate microspore stages).

255   As shown in Figure 1Q–1T, the POD enzyme activity levels (9499–11000 U/g) in the meiosis

256   and microspore tetrad stages were significantly lower in the male sterile line compared with

257   those in the fertile pepper line (11000–13800 U/g). However, the POD enzyme activity levels did

258   not differ significantly in the male sterile and fertile pepper lines in the uninucleate microspore

259   stage. The SOD enzyme activity levels and malondialdehyde contents did not differ significantly

260   in the three stages in the male sterile and fertile pepper lines. In addition, the CAT enzyme

261   activity was significantly lower in the fertile line in the three anther development stages

262   compared with the male sterile pepper line, but especially in the uninucleate microspore stage.

263

264   **Plant hormone contents in different anther development stages in male sterile and fertile**

265   **pepper lines**

266   A previous study determined significant differences in the plant endogenous hormone contents

267   between male sterile and fertile lines in different species (Ding et al. 2018; Yang et al. 2020).

268   Thus, in order to determine whether plant hormones are involved in differential anther

269   development, the gibberellin, auxin, abscisic acid (ABA), and jasmonic acid contents were

270 quantified in the male sterile and fertile pepper lines. As shown in Figure 1U–1X, the gibberellin

271 and jasmonic acid contents were significantly lower in the meiosis stage in the male sterile line

272 compared with the fertile pepper line. In the microspore tetrad stage, the ABA content was

273 slightly higher in the fertile pepper line but the same in the uninucleate microspore stage (Figure

274 1W). However, the auxin content was significantly lower in the uninucleate microspore stage in

275 the fertile line compared with the male sterile pepper line (Figure 1V).

276

277 **DAPs during anther development**

278 To elucidate the molecular mechanisms related to male sterility, proteomic analysis was

279 conducted to determine the differences between the male sterile and fertile pepper lines. The

280 total proteins were extracted from the sterile and fertile lines in the meiosis, tetrad, and

281 binucleate stages, and subjected to proteomic analysis. The proteomic analysis workflow is

282 shown in Figures 2A and 2B. The good repeatability of samples indicates that the result data is

283 highly reliable (Figure 2C). In total, 8516 proteins and 1646 DAPs were identified in all of the

284 samples (Figure 2D and Table S1). The distributions of all DAPs and their overlapping in

285 different developmental stages were visualized by venn diagram analysis. As shown in Figure 3,

286 only eight DAPs (five upregulated and three downregulated) were identified in three stages

287 (Figures 3A and 3B). However, the number DAPs of their overlapping in two different

288 developmental stages were no more than 50 in venn diagram (Figures 3A and 3B). To identify

289 proteins related to male sterility, 362 (213 upregulated and 149 downregulated), 179 (99

290 upregulated and 80 downregulated), and 1104 (453 upregulated and 651 downregulated) DAPs

291 were screened based on comparisons of BY_JS (meiosis stage in the male sterile) vs KY_JS

292 (meiosis stage in the male fertile), BY_SF vs KY_SF (microspore tetrad stage), and BY_SH vs

293 KY_SH (binucleate microspore stage) with fold changes of 1.3 and $P \leq 0.05$ (Figure 3C–3E).

294 The number of DAPs was significantly higher in the binucleate microspore stage than that the

295 meiosis and microspore tetrad stages (Figure 3E).

296

GO analysis of DAPs

298   To clarify the functional categories for DAPs in the male sterile and fertile pepper lines, the
299   DAPs were assigned to three categories comprising biological process, cellular component, and
300   molecular function (Figure 4). Cellular process, metabolic process, and response to stimulus
301   were the most highly enriched terms in all three stages in the biological process category, but
302   especially in the binucleate microspore stage, and the numbers of DAPs assigned to other terms
303   were slightly lower (Figure 4). Interestingly, more DAPs were mainly assigned to peroxisome
304   and microbody process in the microspore tetrad stage (Figures 4 and S1). In the cellular
305   component category, DAPs were significantly enriched in the cell, organelle, and membrane
306   terms (Figure 4). Many DAPs were assigned to translation, cytosolic ribosome process, and
307   amide biosynthesis in the meiosis stage (Figure S1). However, less DAPS were assigned to the
308   extracellular region term in the meiosis stage compared with the binucleate microspore and
309   microspore tetrad stages. Catalytic activity and binding were the most highly enriched molecular
310   function terms in all three stages (Figure 4).

311   The functional subcategories and metabolic pathways were assigned for DAPs, and the results
312   indicated that DAPs in the meiosis stage were mainly enriched in the protein processing in
313   endoplasmic reticulum, proteomic regulatory subunits, and heat shock proteins pathways (Figure
314   5, Supplementary Table S2). In the microspore tetrad stage, the DAPs were mainly enriched in
315   the monoterpenoid biosynthesis pathway. However, the monoterpenoid biosynthesis and starch
316   and sucrose metabolism pathways were enriched in the binucleate microspore stage (Figure 5).

317

Subcellular localizations and domain enrichment analysis for DAPs

319   We also analyzed the subcellular compartment localizations of the DAPs, i.e., cytoplasm,
320   chloroplast, nucleus, plasma membrane, extracellular region, mitochondrion, vacuolar membrane,

321   and endoplasmic reticulum. As shown in Figure 6, the DAPs in all three stages were localized in

322   the cytoplasm, chloroplast, and nucleus, which accounted for 20–30% of the total, thereby

323   demonstrating that proteins in these three compartments had important roles in the male sterile

324   and fertile lines. Interestingly, the distributions of the DAPs mainly differed in the chloroplast

325   and cytoplasm. More DAPs were localized in the cytoplasm (29%) in the meiosis stage

326   compared with the microspore tetrad stage (24%) and binucleate microspore stage (26%) (Figure

327   6A). However, more DAPs were localized in chloroplasts in the microspore tetrad stage (30%)

328   and binucleate microspore stage (31%) compared with the meiosis stage (25%) (Figures 6B, 6C).

329   These different distributions indicate that many proteins in chloroplast compartments affected

330   pollen development in the microspore tetrad and binucleate microspore stages.

331   Protein domain analysis was performed at $P < 0.05$ using the InterPro database. In the BY_JS

332   vs KY_JS comparison, the enriched domains for DAPs included alpha/beta hydrolase fold, NB-

333   ARC, and PIC domains (Figure 6D), whereas most DAPs contained protease inhibitor and

334   trypsin domains in BY_SF vs KY_SF, and all were upregulated proteins (Figure 6E). In BY_SH

335   vs KY_SH, the enriched domains included trypsin and protease inhibitor, PIC, and glycosyl

336   hydrolase domains (Figure 6F). Interestingly, the DAPs containing trypsin and protease inhibitor

337   domains or glycosyl hydrolase domains were upregulated proteins, whereas the DAPs containing

338   PIC domains were downregulated (Supplementary Table S2).

339

340   **PPI networks and cluster analysis**

341   To understand the relationships among DAPs, we determined the PPI networks in different

342   stages using the STRING 11.0 database. For BY_JS vs KY_JS, 14 upregulated proteins

343   (A0A2G2YPH5, A0A2G3AGR1, A0A1U8FF28, and others) were assigned to a ribosome

344   network, and six upregulated proteins and one downregulated protein were clustered in a

345   proteomic interaction network (Figure 7A). However, only 19 DAPs comprised one small

346   network with 13 upregulated proteins and six downregulated proteins for BY_SF vs KY_SF

347 (Figure 7B). In addition, more than 100 proteins in metabolic pathways, TCA cycle

348 (tricarboxylic acid cycle), ribosome, and basal transcription factor established a large and

349 complex interaction network, which was closely related to plant male sterility for BY_SH vs

350 KY_SH (Figure 7C). These PPI networks indicate that anther development is regulated by a

351 complex network.

352 Based on their similar expression patterns, all of the DAPs identified during anther

353 development were divided into six clusters (Figure 8). The expression levels of cluster 2

354 members in the sterile group (BY_JS, BY_SF, and BY_SH) were upregulated compared with

355 those in the fertile group (KY_JS, KY_SF, and KY_SH), but the expression levels of cluster 1

356 members in the sterile group (BY_JS, BY_SF, and BY_SH) were downpregulated compared

357 with those in the fertile group (KY_JS, KY_SF, and KY_SH) (Figure 8). Furthermore, these

358 DAPs were mainly related to citrate metabolic process, cold acclimation, regulatory region

359 nucleic acid binding, response to jasmonic acid, microbody, and acid phosphatase activity

360 pathway (Figures 8 and S2). Furthermore, the expression levels in cluster 5 were significantly

361 downregulated in KY_SH compared with BY_SH, whereas those of some in cluster 6 were

362 upregulated in KY_SH, where they were involved in response to stress, stimulus, peroxisome,

363 antioxidant activity, detoxification, and other metabolism pathways (Figures 8 and S2).

364

365 Targeted protein quantification by PRM

366 To confirm the reliability of the proteome data, PRM was conducted to quantify the targeted

367 proteins. About 15–20 proteins from the KEGG pathway data in three different stages were

368 randomly selected and quantified. Nineteen proteins from 20 selected randomly in the meiosis

369 stage (BY_JS vs KY_JS) had quantitative information and 1.5-fold changes occurred in all of

370 these proteins, where 13 were downregulated and six were upregulated (Figure 9A). Due to the

371 properties of the proteins and their abundances, six proteins (four downregulated and two

372 upregulated) were randomly selected from 15 proteins identified in the microspore tetrad stage

373   (BY_SF vs KY_SF) (Figure 9B). Interestingly, three downregulated proteins with lipid-binding

374   domains comprising A0A2G2YY91, A0A2G3AC90, and A0A1U8E7C6 may function in lipid

375   transport during anther development. In addition, 20 proteins (10 downregulated and 10

376   upregulated) among 22 randomly selected proteins identified as proteins related to

377   glycometabolism, including A0A2G2ZTG5, A0A1U8F8K6, and A0A1U8HAH9, were

378   downregulated in the binucleate microspore stage in the male fertile pepper line (Figure 9C). The

379   PRM results indicate that the DAPs were stable and accurately quantified.

380

381   **DISCUSSION**

382   Due to the higher yields of hybrid crops, heterosis has been used to breed cereals and

383   horticultural plants, including maize, wheat, rice, and vegetable crops. It is generally considered

384   that artificial supplementary pollination is too difficult and expensive for breeding hybrid seeds.

385   Therefore, it is necessary to select male sterile lines to accelerate the propagation of hybrid seeds

386   (Wang et al. 2019). In this study, we screened one male sterile pepper line and identified a set of

387   typical features associated with male sterility, where the tapetal layer collapsed and disintegrated

388   microspores adhered to the tapetum in a dense belt according to cytological observation. This

389   phenomenon may be responsible for pollen abortion, as shown in previous studies (Guo et al.

390   2017; Han et al. 2018). However, the genes that control these traits and the molecular mechanism

391   responsible for pollen abortion in pepper are still unclear.

392   Proteomic analysis is an efficient and reliable method, and it has been applied widely to

393   understand pollen formation and development in plants. Recent studies have shown that pollen

394   abortion in monocotyledons generally occurs in the uninucleate and binucleate microspore stages,

395   whereas pollen abortion in dicotyledons typically occurs in the microspore tetrad stage (Guo et al.

396   2017; Han et al. 2018). In the present study, we conducted proteomic analysis to detect

397   differences in DAPs in the meiosis, microspore tetrad, and binucleate microspore stages during

398   anther development. In total, 362 (213 upregulated and 149 downregulated), 179 (99 upregulated

399 and 80 downregulated), and 1104 (453 upregulated and 651 downregulated) DAPs were

400 identified in the meiosis, tetrad, and binucleate stages, respectively, which were enriched mainly

401 in monoterpenoid biosynthesis, and starch and sucrose metabolism pathways. According to

402 KEGG analysis, monoterpenoid biosynthesis and starch and sucrose metabolism were enriched

403 in the binucleate microspore stage. Furthermore, glucosidase proteins related to starch and

404 sucrose synthesis were upregulated in the fertile pepper line. Differences in the accumulation and

405 metabolism of amino acids, monoterpenoids, and sugars are closely related to pollen abortion in

406 fertile and sterile plant lines (Zheng et al. 2014). In the present study, many proteins related to

407 glycometabolism were quantified as downregulated by PRM, thereby indicating that a lack of the

408 glucose molecules required for biosynthesis and energy balance maintenance may contribute to

409 pollen abortion in male sterile plants. Carbohydrate metabolism is one of the most basic

410 metabolic pathways for providing energy and carbon sources in the whole plant life cycle (Wu et

411 al. 2013). The levels of lipid transport-related proteins were also significantly reduced in the

412 male sterile plant line, and they may play important roles in cuticle deposition on the walls of

413 expanding epidermal cells in the tetrad stage. Exine formation is required for the absorption of

414 essential nutrients (sugars, amino acids, and other sources) and the release of microspores from

415 the tetrad during anther development (Chang et al. 2016b; Yang et al. 2019). Furthermore, the

416 subcellular compartments of DAPs were identified, where most were localized in chloroplasts in

417 the microspore tetrad and binucleate microspore stages, thereby indicating that chloroplast

418 proteins have key roles in anther development. It is well known that carbohydrate metabolism,

419 antioxidant reactions, photosynthesis, and plant hormone synthesis occur in chloroplasts (Chu et

420 al. 2015; Jo et al. 2009; Kurepa & Smalle 2019). UDP-glucose 4-epimerase 3 is involved in

421 galactose metabolism and it was downregulated in the male sterile line, thereby suggesting that

422 the tricarboxylic acid cycle, photosynthesis, and glycometabolism were less active, thereby

423 contributing to male sterility. These new candidates related to male sterility may facilitate the

424 cloning of key factors associated with male sterility in future research.

425 Male sterility is also associated with energy metabolism disorders, the accumulation of

426 reactive oxygen species (ROS), programmed cell death, and glycolysis in male sterile wheat

427 according to proteomic analysis of pollen (Zhang et al. 2016). Previous studies have

428 demonstrated that programmed cell death and ROS stress occur in the tapetum to affect the

429 provision of nutrients and metabolites for microspore development in male sterility (Ariizumi &

430 Toriyama 2007; Guo et al. 2017). The tapetal layer is essential for pollen grain development

431 because it is the site of synthesis for proteins, which are then transported to the anther walls (Qiu

432 et al. 2016; Yang et al. 2014). Male sterility in *Arabidopsis thaliana* is associated with

433 microspore development due to premature or delayed tapetal programmed cell death (Ariizumi &

434 Toriyama 2007). Our morphological observations indicated the occurrence of premature death

435 and vacuolation with the crushing of the microspores in the tapetal stage in the male sterile line,

436 thereby leading to callosum degradation and microspore release in the uninucleate stage (Fig. 2).

437 The dynamic balance between enzymatic and nonenzymatic systems in plant cells allows

438 antioxidant enzymes such as POD, CAT, SOD, and ascorbate peroxidase to eliminate ROS. In

439 this study, we detected the activities of antioxidant enzymes (SOD, POD, and CAT) and found

440 that the activities of all were significantly lower in the male sterile line than the fertile line,

441 thereby indicating that excess ROS could not be removed in the meiosis and microspore tetrad

442 stages. Excess ROS leads to programmed cell death and peroxidation of plant membrane lipids

443 (Geng et al. 2018). We suggest that ROS may trigger programmed cell death and lead to male

444 sterility in the pepper line. In addition, phytohormones are now recognized as vital factors that

445 regulate plant development and growth, reproductive processes, biotic and abiotic stress

446 responses, and tissue senescence (Bleecker & Kende 2000; Zhao et al. 2021a). Previous studies

447 have identified the specific roles of plant endogenous hormones in male sterility and fertility

448 (Dubas et al. 2013; Shukla & Sawhney 1994). Therefore, we assessed phytohormones in the

449 male sterile and fertile lines to detect any differences. We found significant differences in the

450 endogenous ABA, auxin, and gibberellin contents in different bud development stages. The ABA

451 concentration was higher in younger floral buds. The different ABA contents may affect plant

452 pollen abortion by specifically blocking the transport of apoplastic sugars and other

453 carbohydrates during pollen development (Ding et al. 2018). The tomato male sterile line jai1-1

454 is a mutant with defective jasmonic acid perception, where SlMYB21 positively regulates

455 jasmonic acid biosynthesis but negatively regulates auxin and gibberellin (Schubert et al. 2019).

456 The overexpression of AtMYB2, which is the target of JAZ repressors, can also partially rescue

457 male fertility in *Arabidopsis* stamen and pollen development (Song et al. 2011). In general,

458 phytohormones and antioxidant enzymes are key factors that regulate male sterility in pollen

459 development.

460 **CONCLUSIONS**

461 In this study, we employed cytological analysis, bioinformatics, proteomics, and plant

462 physiological assays to gain insights into the mechanisms associated with male sterility in pepper.

463 We screened 1645 DAPs from a male sterile pepper line based on proteome analyses and 45

464 DAPs were quantitatively identified in the meiosis, tetrad, and binucleate stages by PRM, which

465 were related to monoterpenoid biosynthesis, and starch and sucrose metabolism pathways. The

466 DAPs were mainly distributed in the chloroplast and cytoplasm. In addition, the POD and CAT

467 enzyme activities were significantly lower in the male sterile line compared with the fertile line,

468 and the gibberellin, jasmonic acid, and auxin contents also differed. The results obtained in this

469 study improve our understanding of the essential factors related to pollen development in male

470 sterility.

471

472 **Funding**

473 This study was funded by the Agricultural Science and Technology Innovation Fund of Ningxia

474 (NGSB-2021-8-01), National Natural Science Foundation of China (31860555), and National

475 Natural Science Foundation of Ningxia (2021A1237).

476

477 **Competing Interests**

478 The authors declare that they have no competing interests.

479

480 **Author Contributions**

481 Author Contributions: For research articles with several authors, a short paragraph specifying
482 their individual contributions must be provided. The following statements should be used
483 "**Conceptualization, Hongxia Pei, Jingxia Gao, and Jie Gao; methodology, Hongxia Pei,**
484 **Hua Xie, Xuemei Wang, and Xiujuan Yan; software, Baike Wang, and Haiping Feng;**
485 **validation, Hongxia Pei, Jingxia Gao, and Jie Gao; formal analysis, Hongxia Pei, and**
486 **Yunxia Zhao; investigation, Hongxia Pei, and Hua Xie; resources, Hua Xie, Xuemei Wang,**
487 **and Jingxia Gao; data curation, Hua Xie, Xiujuan Yan, and Baike Wang; writing—**
488 **original draft preparation, Hongxia Pei, Haiping Feng, and Yunxia Zhao; writing—review**
489 **and editing, Hongxia Pei, Jingxia Gao, and Jie Gao; visualization, Hua Xie; supervision,**
490 **Jingxia Gao, and Jie Gao; project administration, Jingxia Gao, and Jie Gao; funding**
491 **acquisition, Jingxia Gao, and Baike Wang. All authors have read and agreed to the**
492 **published version of the manuscript**."

493

494

495

496

497 **References**

498 Ariizumi T, and Toriyama K. 2007. Pollen Exine Pattern Formation is Dependent on Three Major
499   Developmental Processes in *Arabidopsis thaliana*. *The International Journal of Developmental*
500   *Biology* 1:106–115.

501   Ariizumi T, and Toriyama K. 2011. Genetic regulation of sporopollenin synthesis and pollen exine
502   development. *Annual Review of Plant Biology* 62:437-460. 10.1146/annurev-arplant-042809-112312

503   Arimura S, Ayabe H, Sugaya H, Okuno M, Tamura Y, Tsuruta Y, Watari Y, Yanase S, Yamauchi T, Itoh T, Toyoda
504   A, Takanashi H, and Tsutsumi N. 2020. Targeted gene disruption of ATP synthases 6-1 and 6-2 in the
505   mitochondrial genome of *Arabidopsis thaliana* by mitoTALENs. *Plant Journal* 104:1459-1471.
506   10.1111/tpj.15041

507   Blackmore S, Wortley A, Skvarla J, and Rowley J. 2007. Pollen wall development in flowering plants. *New
508   phytologist* 174:483-498. 10.1111/j.1469-8137.2007.02060.x

509   Bleecker AB, and Kende H. 2000. Ethylene: a gaseous signal molecule in plants. *Annual Review of Cell &
510   Developmental Biology* 16:1-18.

511   Bohra A, Jha U, Adhimoolam P, Bisht D, and Singh N. 2016. Cytoplasmic male sterility (CMS) in hybrid
512   breeding in field crops. *Plant Cell Reports* 35:967-993. 10.1007/s00299-016-1949-3

513   Chang Z, Chen Z, Wang N, Xie G, Lu J, Yan W, Zhou J, Tang X, and Deng X. 2016a. Construction of a male
514   sterility system for hybrid rice breeding and seed production using a nuclear male sterility gene. *Proc
515   Natl Acad Sci U S A* 113:14145-14150. 10.1073/pnas.1613792113

516   Chang Z, Chen Z, Yan W, Xie G, Lu J, Wang N, Lu Q, Yao N, Yang G, and Xia J. 2016b. An ABC transporter,
517   OsABCG26, is required for anther cuticle and pollen exine formation and pollen-pistil interactions in
518   rice. *Plant Science* 253.

519   Chen, C., Chen, H., Zhang, Y.i., Thomas, H.R., Frank, M.H., He, Y., Xia, R., 2020. TBtools: An integrative toolkit
520   developed for interactive analyses of big biological data. *Molecular Plant* 13 (8), 1194－1202.

521   Cheng X, Zhang X, Xue F, Zhu S, Li Y, Zhu Q, Liu F, and Sun J. 2020. Characterization and transcriptome analysis
522   of a dominant genic male sterile cotton mutant. *BMC Plant Biology* 20:312. 10.1186/s12870-020-
523   02522-0.

524   Cheng, Q.; Li, T.; Ai, Y.; Lu, Q.; Wang, Y.; Sun, L.; Shen, H. 2019. Complementary transcriptomic and proteomic
525   analysis reveals a complex network regulating pollen abortion in GMS (msc-1) pepper (*Capsicum
526   annuum* L.). *International Journal of Molecular Sciences* 20, 1789.
527   https://doi.org/10.3390/ijms20071789.

528   Chu P, Yan GX, Yang Q, Zhai LN, Zhang C, Zhang FQ, and Guan RZ. 2015. ITRAQ-based quantitative proteomics
529   analysis of *Brassica napus* leaves reveals pathways associated with chlorophyll deficiency. *Journal of
530   proteomics* 113:244-259.

531   Ding B, Hao M, Mei D, Zaman Q, Sang S, Wang H, Wang W, Fu L, Cheng H, and Hu Q. 2018. Transcriptome and
532   hormone comparison of three cytoplasmic male sterile systems in *Brassica napus*. *International*
533   *Journal of Molecular Sciences* 19. 10.3390/ijms19124022

534   Dubas E, Janowiak F, Krzewska M, and Hura… T. 2013. Endogenous ABA concentration and cytoplasmic
535   membrane fluidity in microspores of oilseed rape (*Brassica napus* L.) genotypes differing in
536   responsiveness to androgenesis induction. *Plant Cell Reports* 32:1465-1475.

537   Durand S, Ricou A, Simon M, Dehaene N, Budar F, and Camilleri C. 2021. A restorer-of-fertility-like
538   pentatricopeptide repeat protein promotes cytoplasmic male sterility in *Arabidopsis thaliana*. *The*
539   *Plant Journal* 105:124-135. https://doi.org/10.1111/tpj.15045

540   Geng X, Ye J, Yang X, Sha L, Zhang L, and Song X. 2018. Identification of proteins involved in carbohydrate
541   metabolism and energy metabolism pathways and their regulation of cytoplasmic male sterility in
542   wheat. *International Journal of Molecular Sciences* 19:324-.

543   Geyer M, Bund A, Albrecht T, Hartl L, and Mohler V. 2016. Distribution of the fertility-restoring gene *Rf3* in
544   common and spelt wheat determined by an informative SNP marker. *Molecular Breeding* 36:167.

545   Gulyas G, Shin Y, Kim H, Lee J-S, and Hirata Y. 2010. Altered transcript reveals an *Orf 507* sterility-related gene
546   in chili pepper (*Capsicum annuum* L.). *Plant Molecular Biology Reporter* 28:605-612. 10.1007/s11105-
547   010-0182-4

548   Guo J, Liu C, Wang P, Cheng Q, Sun L, Yang W, and Shen H. 2018. Aborted microspores the (AMS)-like gene is
549   required for anther and microspore development in pepper (*Capsicum annuum* L.). *International*
550   *Journal of Molecular Sciences* 19. 10.3390/ijms19051341

551   Guo J, Wang P, Cheng Q, Sun L, Wang H, Wang Y, Kao L, Li Y, Qiu T, Yang W, and Shen H. 2017. Proteomic
552   analysis reveals strong mitochondrial involvement in cytoplasmic male sterility of pepper (*Capsicum*
553   *annuum* L.). *Journal of proteomics* 168:15-27. 10.1016/j.jprot.2017.08.013

554   Han F, Zhang X, Yang L, Zhuang M, Zhang Y, Li Z, Fang Z, and Lv H. 2018. iTRAQ-based proteomic analysis of
555   Ogura-CMS cabbage and its maintainer line. *International Journal of Molecular Sciences* 19.

556   Jo YD, Jeong HJ, and Kang BC. 2009. Development of a CMS-specific marker based on chloroplast-derived
557   mitochondrial sequence in pepper. *Plant Biotechnology Reports* 3:309-315.

558   Kim D, and Kim B. 2006. The organization of mitochondrial *atp6* gene region in male fertile and CMS lines of
559   pepper (*Capsicum annuum* L.). *Current Genetics* 49:59-67. 10.1007/s00294-005-0032-3.

560   Kurepa J, and Smalle JA. 2019. Oxidative stress-induced formation of covalently linked ribulose-1,5-

561   bisphosphate carboxylase/oxygenase large subunit dimer in tobacco plants. *Bmc Research Notes* 12.

562   Liu S, Liu Y, Yang X, Tong C, Edwards D, Parkin I, Zhao M, Ma J, Yu J, Huang S, Wang X, Wang J, Lu K, Fang Z,
563   Bancroft I, Yang T, Hu Q, Wang X, Yue Z, Li H, Yang L, Wu J, Zhou Q, Wang W, King G, Pires J, Lu C, Wu
564   Z, Sampath P, Wang Z, Guo H, Pan S, Yang L, Min J, Zhang D, Jin D, Li W, Belcram H, Tu J, Guan M, Qi
565   C, Du D, Li J, Jiang L, Batley J, Sharpe A, Park B, Ruperao P, Cheng F, Waminal N, Huang Y, Dong C,
566   Wang L, Li J, Hu Z, Zhuang M, Huang Y, Huang J, Shi J, Mei D, Liu J, Lee T, Wang J, Jin H, Li Z, Li X,
567   Zhang J, Xiao L, Zhou Y, Liu Z, Liu X, Qin R, Tang X, Liu W, Wang Y, Zhang Y, Lee J, Kim H, Denoeud F,
568   Xu X, Liang X, Hua W, Wang X, Wang J, Chalhoub B, and Paterson A. 2014. The *Brassica oleracea*
569   genome reveals the asymmetrical evolution of polyploid genomes. *Nature Communications* 5:3930.
570   10.1038/ncomms4930.

571   Lou P, Kang J, Zhang G, Bonnema G, Fang Z, and Wang X. 2007. Transcript profiling of a dominant male sterile
572   mutant (*Ms-cd1*) in cabbage during flower bud development. *Plant Science* 172:111-119.
573   https://doi.org/10.1016/j.plantsci.2006.07.015.

574   Melonek J, Duarte J, Martin J, Beuf L, Murigneux A, Varenne P, Comadran J, Specel S, Levadoux S, Bernath-
575   Levin K, Torney F, Pichon J, Perez P, and Small I. 2021. The genetic basis of cytoplasmic male sterility
576   and fertility restoration in wheat. *Nature Communications* 12:1036. 10.1038/s41467-021-21225-0.

577   Ning L, Wang H, Li D, Lin Z, Li Y, Zhao W, Chao H, Miao L, and Li M. 2019. Transcriptomic and proteomic
578   analysis of Shaan2A cytoplasmic male sterility and its maintainer line in *Brassica napus*. *Front Plant*
579   *Sci* 10:252. 10.3389/fpls.2019.00252.

580   Qiu Y, Liao L, Jin X, Mao D, and Liu R. 2018. Analysis of the meiotic transcriptome reveals the genes related to
581   the regulation of pollen abortion in cytoplasmic male-sterile pepper (*Capsicum annuum* L.). *Gene*
582   641:8-17. 10.1016/j.gene.2017.10.022.

583   Qiu Y, Liao L, Liu S, Mao D, and Liu R. 2016. Differences on the microsporogenesis and tapetal development of
584   male fertile and cytoplasmic male sterile pepper (*Capsicum annuum* L.). *Grana* 56:1-13.

585   Schubert R, Dobritzsch S, Gruber C, Hause G, Athmer B, Schreiber T, Marillonnet S, Okabe Y, Ezura H, Acosta I,
586   Tarkowska D, and Hause B. 2019. Tomato *MYB21* acts in ovules to mediate jasmonate-regulated
587   fertility. *Plant Cell* 31:1043-1062. 10.1105/tpc.18.00978.

588   Sheoran I, and Sawhney V. 2010. Proteome analysis of the normal and Ogura (ogu) CMS anthers of *Brassica*
589   *napus* to identify proteins associated with male sterility. *Botany* 88:217-230. 10.1139/B09-085.

590   Shukla A, and Sawhney VK. 1994. Abscisic acid: one of the factors affecting male sterility in *Brassica napus*.
591   *Physiologia Plantarum* 91.

592   Song S, Qi T, Huang H, Ren Q, Wu D, Chang C, Peng W, Liu Y, Peng J, and Xie D. 2011. The jasmonate-ZIM
593   domain proteins interact with the R2R3-MYB transcription factors MYB21 and MYB24 to affect
594   jasmonate-regulated stamen development in *Arabidopsis*. *Plant Cell* 23:1000-1013.

595   Song S, Wang T, Li Y, Hu J, Kan R, Qiu M, Deng Y, Liu P, Zhang L, Dong H, Li C, Yu D, Li X, Yuan D, Yuan L, and Li
596   L. 2021. A novel strategy for creating a new system of third-generation hybrid rice technology using a
597   cytoplasmic sterility gene and a genic male-sterile gene. *Plant Biotechnology Journal* 19:251-260.
598   https://doi.org/10.1111/pbi.13457

599   Tang H, Xie Y, Liu Y, and Chen L. 2017. Advances in understanding the molecular mechanisms of cytoplasmic
600   male sterility and restoration in rice. *Plant reproduction* 30:179-184. 10.1007/s00497-017-0308-z.

601   van der Linde K, and Walbot V. 2019. Pre-meiotic anther development. *Current topics in developmental
602   biology* 131:239-256. 10.1016/bs.ctdb.2018.11.001.

603   Wang P, Lu Q, Ai Y, Wang Y, Li T, Wu L, Liu J, Cheng Q, Sun L, and Shen H. 2019. *Capsicum annuum* candidate
604   gene selection for cytoplasmic male sterility in pepper (*Capsicum annuum* L.) through whole
605   mitochondrial genome sequencing. *International Journal of Molecular Sciences* 20.
606   10.3390/ijms20030578.

607   Wei B, Wang L, Bosland PW, Zhang G, and Zhang R. 2019. Comparative transcriptional analysis of *Capsicum
608   flower buds between a sterile flower pool and a restorer flower pool provides insight into the
609   regulation of fertility restoration. *BMC genomics* 20:837. 10.1186/s12864-019-6210-3.

610   Wen L, Liu G, Li S-Q, Wan C-X, Tao J, Xu K-Y, Zhang Z-J, and Zhu Y-G. 2007. Proteomic analysis of anthers from
611   Honglian cytoplasmic male sterility line rice and its corresponding maintainer and hybrid. *Botanical
612   Studies* 48.

613   Wu Z, Cheng J, Qin C, Hu Z, Yin C, and Hu K. 2013. Differential proteomic analysis of anthers between
614   cytoplasmic male sterile and maintainer lines in *capsicum annuum* L. *International Journal of
615   Molecular Sciences* 14:22982-22996.

616   Yang X, Ye J, Zhang L, and Song X. 2020. Blocked synthesis of sporopollenin and jasmonic acid leads to pollen
617   wall defects and anther indehiscence in genic male sterile wheat line *4110S* at high temperatures.
618   *Functional & Integrative Genomics* 20:383-396. 10.1007/s10142-019-00722-y.

619   Yang Y, Dong C, Yu J, Shi L, Tong C, Li Z, Huang J, and Liu S. 2014. Cysteine Protease 51 (*CP51*), an anther-
620   specific cysteine protease gene, is essential for pollen exine formation in *Arabidopsis*. *Plant Cell,
621   Tissue and Organ Culture (PCTOC)* 119:383-397. 10.1007/s11240-014-0542-0.

622 Yang Z, Liu L, Sun L, Yu P, Zhang P, Abbas A, Xiang X, Wu W, Zhang Y, and Cao L. 2019. OsMS1 functions as a
623   transcriptional activator to regulate programmed tapetum development and pollen exine formation
624   in rice. *Plant Molecular Biology. 10.1007/s11103-018-0811-0.*

625 Yuan Q, Song C, Gao L, Zhang H, Yang C, Sheng J, Ren J, Chen D, and Wang Y. 2018. Transcriptome de novo
626   assembly and analysis of differentially expressed genes related to cytoplasmic male sterility in onion.
627   *Plant physiology and biochemistry* 125:35-44. 10.1016/j.plaphy.2018.01.015.

628 Zhang F, Li G, Ding Q, Wang Z, Ma X, Zhang H, Zhang Z, Jin F, and Ma L. 2016. Proteome analysis of pollen in
629   the K-type male sterility line *732A* and its maintainer *732B* in wheat (*Triticum aestivum* L.) by two-
630   dimensional gel electrophoresis. *Acta Physiologiae Plantarum* 38:84.

631 Zhang G, Ye J, Jia Y, Zhang L, and Song X. 2018. iTRAQ-based proteomics analyses of sterile/fertile anthers
632   from a thermo-sensitive cytoplasmic male-sterile wheat with *Aegilops kotschyi* cytoplasm.
633   *International Journal of Molecular Sciences* 19:1344. 10.3390/ijms19051344

634 Zhao B, Liu Q, Wang B, and Yuan F. 2021a. Roles of phytohormones and their signaling pathways in leaf
635   development and stress responses. *Journal of agricultural and food chemistry*.
636   10.1021/acs.jafc.0c07908.

637 Zhao N, Li Z, Zhang L, Yang X, Mackenzie S, Hu Z, Zhang M, and Yang J. 2021b. MutS HOMOLOG1 mediates
638   fertility reversion from cytoplasmic male sterile *Brassica juncea* in response to environment. *Plant,*
639   *cell & environment* 44:234-246. 10.1111/pce.13895.

640 Zheng BB, Fang YN, Pan ZY, Sun L, Deng XX, Grosser JW, and Guo WW. 2014. iTRAQ-based quantitative
641   proteomics analysis revealed alterations of carbohydrate metabolism pathways and mitochondrial
642   proteins in a male sterile cybrid pummelo. *Journal of Proteome Research* 13:2998.

643

644

Figure 1

Characteristics of anthers in different development stages in male sterile and fertile lines.

A-G:The cytological observation of anthers development stages in fertile lines; H-N: The cytological observation of anthers development stages in male sterile lines. A and H: the sporogenous cell stage; B and I: the pollen mother cell stage;C and J: meiosis stage; D and K: the microspore tetrad stage; E and L: the uninucleate microspore stage; F and M: binucleate microspore stage;G and N: pollen maturation stage. MMC, pollen mother cells; MC, meiotic cell; T, tapetum; Tds, tetrads; Msp, microspore; PG, mature pollen grain; Bar=100 μm. O-P: Pollen grains from male sterile and fertile lines stained by aceto-carmine. Bar=100 μm. Q-T: Detection of antioxidant enzyme activity in meiosis, microspore tetrad and uninucleate microspore stages. U-X: Detection of plant hormone content in meiosis, microspore tetrad and uninucleate microspore stages.

Fertile Line (KY) **Sterile Line (BY)**

Sporogenous cell stage

Pollen mother cell stage

Meiosis stage

Microspore tetrad stage

Uninucleate microspore stage

Binucleate microspore stage

pollen maturation stage

Pollen grain
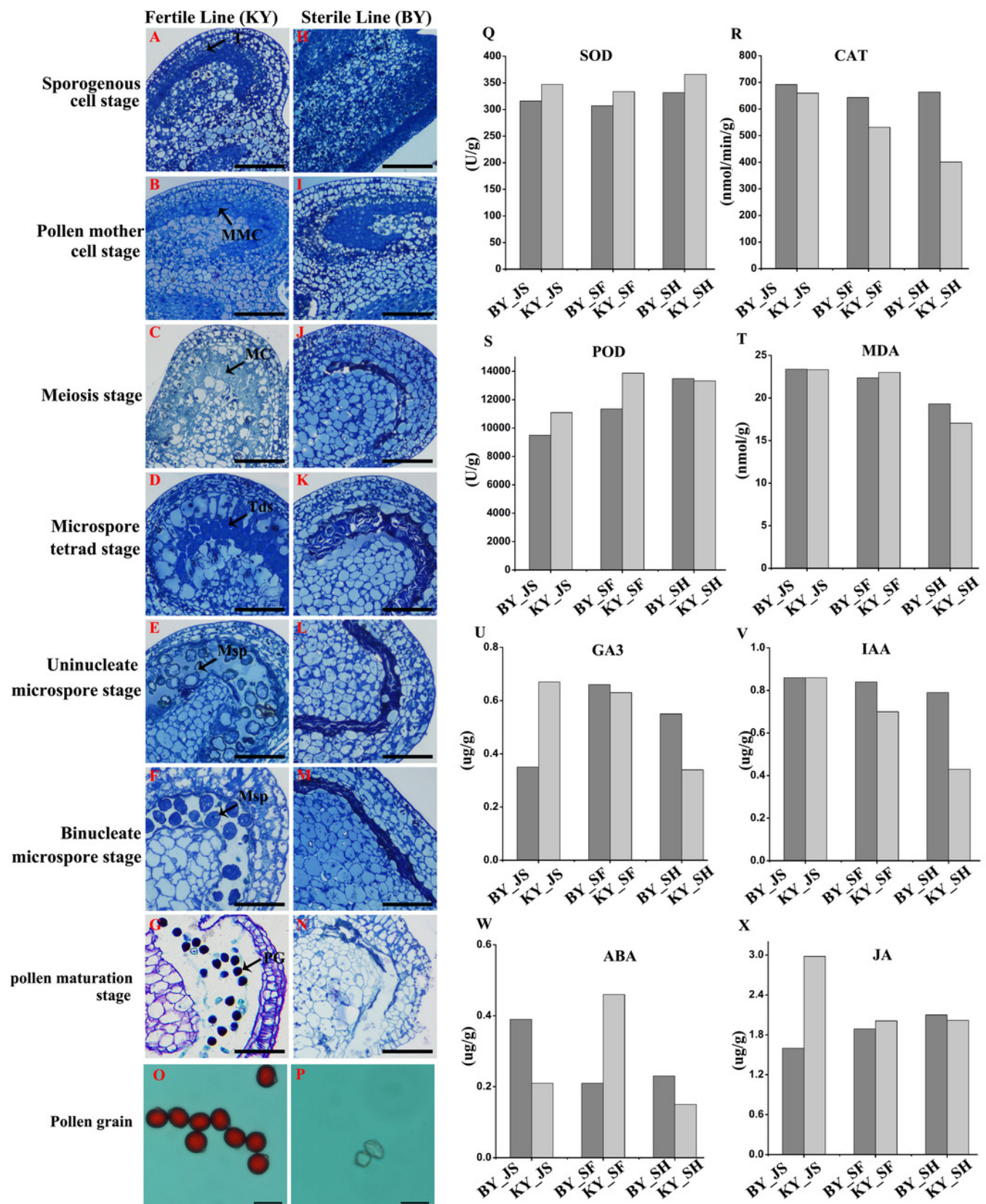
Figure 2

Proteome analysis of anthers at different development stages in the male sterile and fertile lines.

A: Outline of experimental workflow. B: Outline of proteome sequence. C:PCA plots from proteome of anthers in meiosis, tetrad and binucleate stages in the male sterile and fertile lines. D: Statistic of DAPs in meiosis, tetrad and binucleate stages from sterile and fertile line.

A

Sample preparation · Protein extraction Proteolysis · TMT Labeling · LC-MS/MS · Data analysis

Tryptic digestion

B

Total spectrums
n=1097308

↓

Matched spectrum
n=207556

↓

Peptides
n=103387

↓

Modified peptides
n=94006

↓

Identified sites
n=8516

↓

Quantifiable sites
n=8263

C

PC2 (30.9%) vs PC1 (45.0%)

Sample type
- BY_JS
- BY_SF
- BY_SH
- KY_JS
- KY_SF
- KY_SH

D

Type
- Down-regulated
- Up-regulated

	Down-regulated	Up-regulated
BY_JS/KY_JS	149	213
BY_SF/KY_SF	80	99
BY_SH/KY_SH	651	454

Figure 3

Differential abundance proteins (DAPs) in meiosis, tetrad and binucleate stages from sterile and fertile lines.

A-B:Venn diagrams of DAPs between BY_JS vs KY_JS, BY_SF vs KY_SF and BY_SH vs KY_SH; C-E: Volcano plots of the DAPs in meiosis, microspore tetrad and binucleate microspore stages, repectively; JS, meiosis; SF, microspore tetrad; SH, binucleate microspore stages.
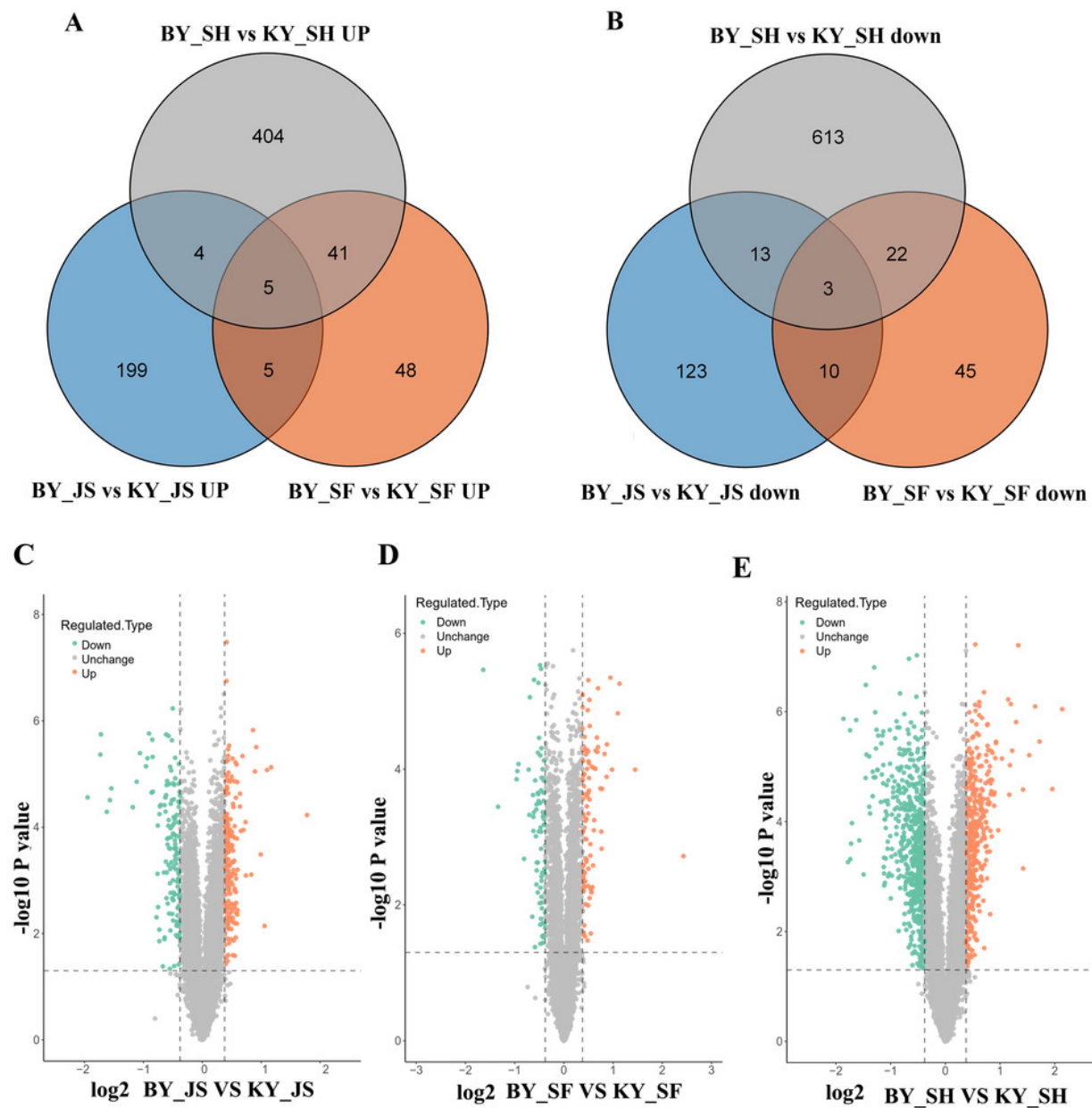
Figure 4

Statistical distribution of DAPs under each GO annotation at meiosis, microspore tetrad and binucleate microspore stages in the male sterile and fertile lines.

A-C: GO terms of DAPs at meiosis, microspore tetrad and binucleate stages in the male sterile and fertile lines, respectively. The x-axis represents GO terms and the y-axis represents the number of DAPs.
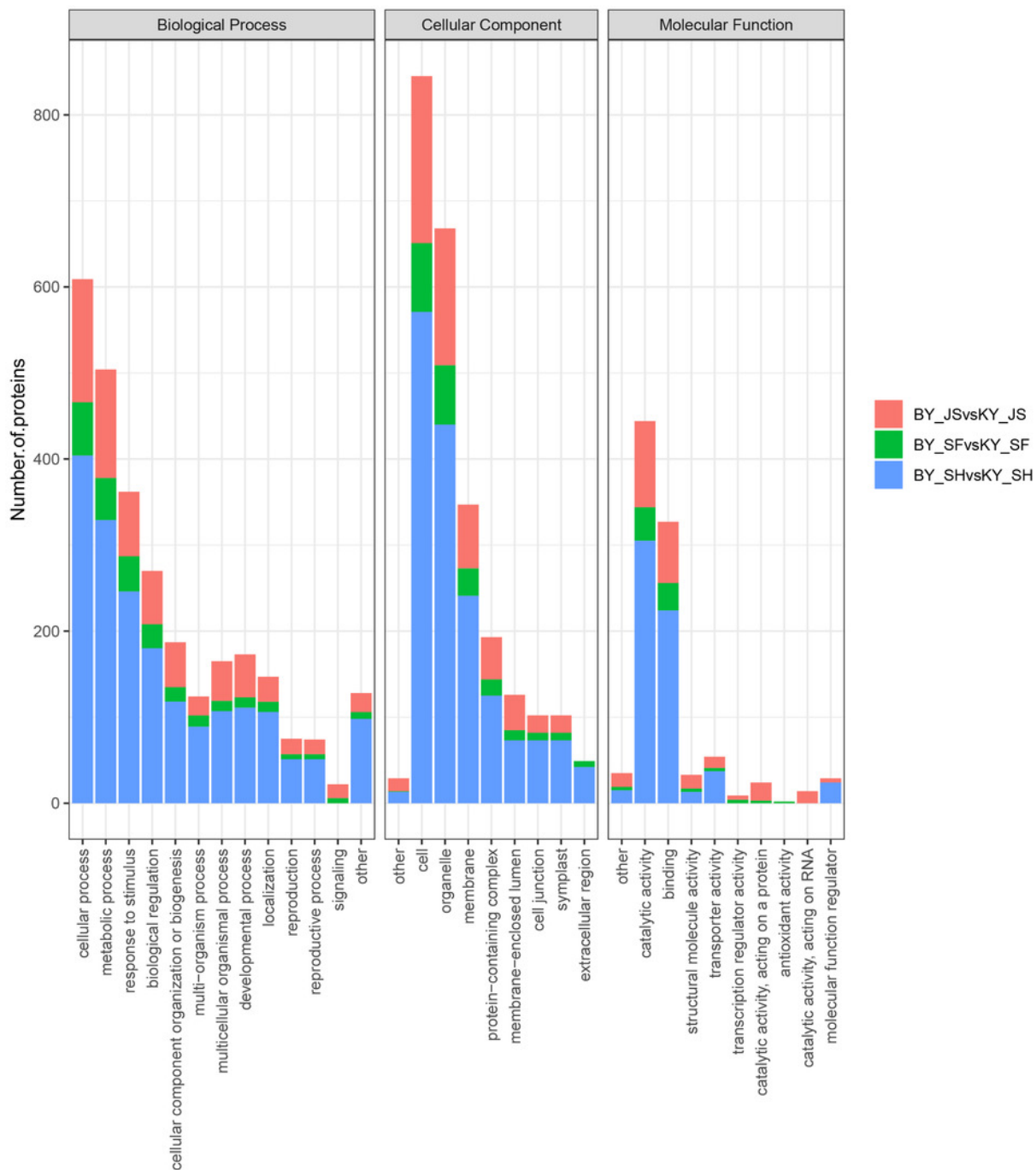
Figure 5

KEGG pathway of DAPs at meiosis, microspore tetrad and binucleate stages between male sterile and fertile lines.

A-C: KEGG pathway for DAPs in the meiosis, microspore tetrad and binucleate stages, respectively.
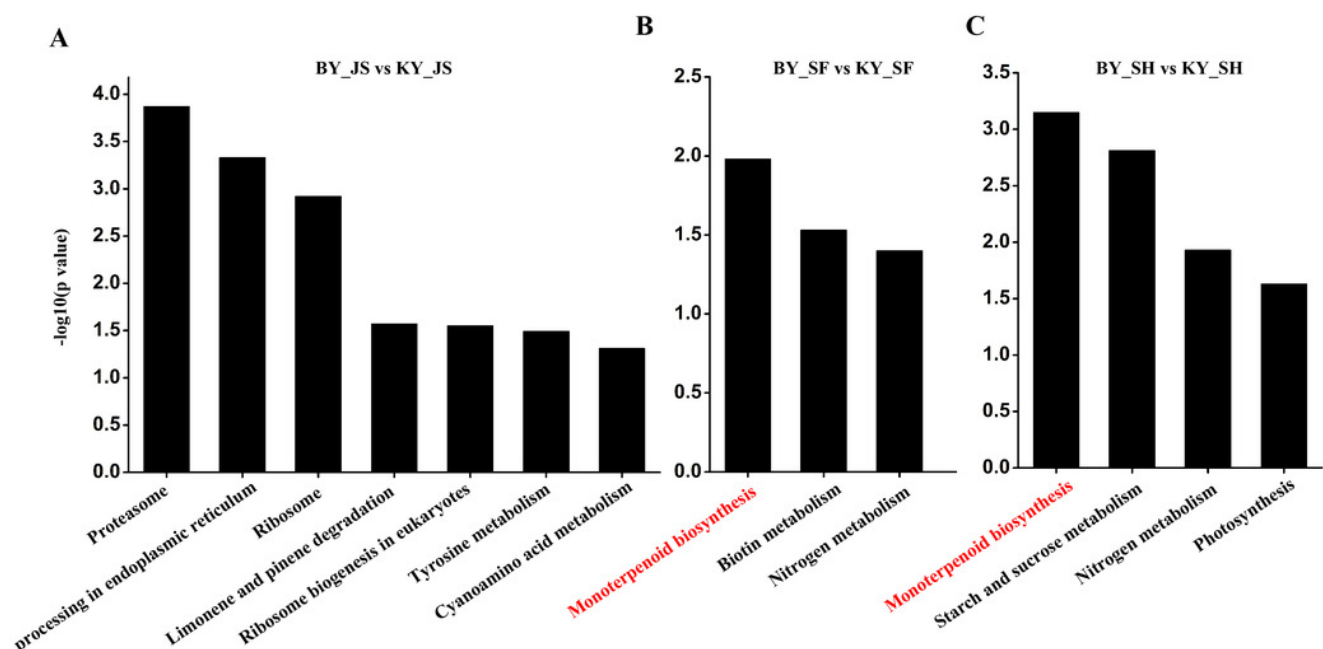
Figure 6

Characteristics of DAPs in the different comparison groups.

A: Subcellular localization of DAPs in BY_JS vs KY_JS. B: Subcellular localization of DAPs in BY_SF vs KY_SF. C: Subcellular localization of DAPs in BY_SH vs KY_SH. D: Enrichment of DAPs in BY_JS vs. KY_JS. E: Enrichment of DAPs in BY_SF vs. KY_SF. F: Enrichment of DAPs in BY_SH vs. KY_SH.
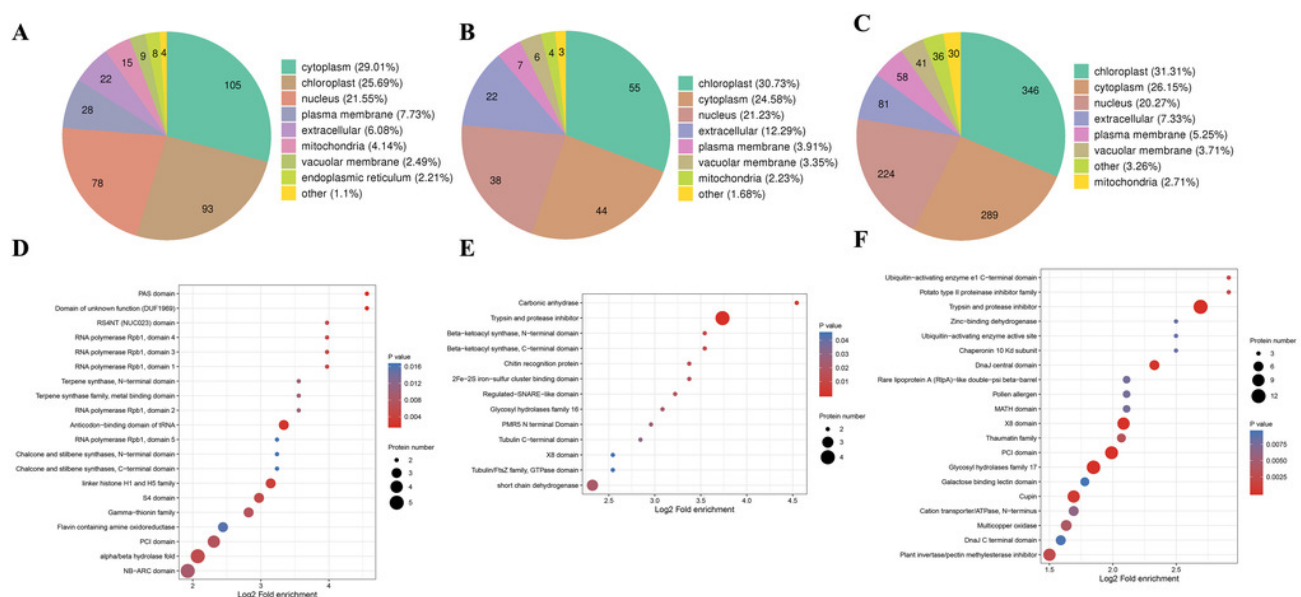
Figure 7

Protein-protein interaction network (PPI) of DAPs.

A: BY_JS vs KY_JS. B: BY_SF vs KY_SF. C: BY_SH vs KY_SH. The network was constructed by the String program (http://www.string-db.org/) with a confidence score higher than 0.4. Nodes represent proteins and the line thickness represents the strength in the picture.
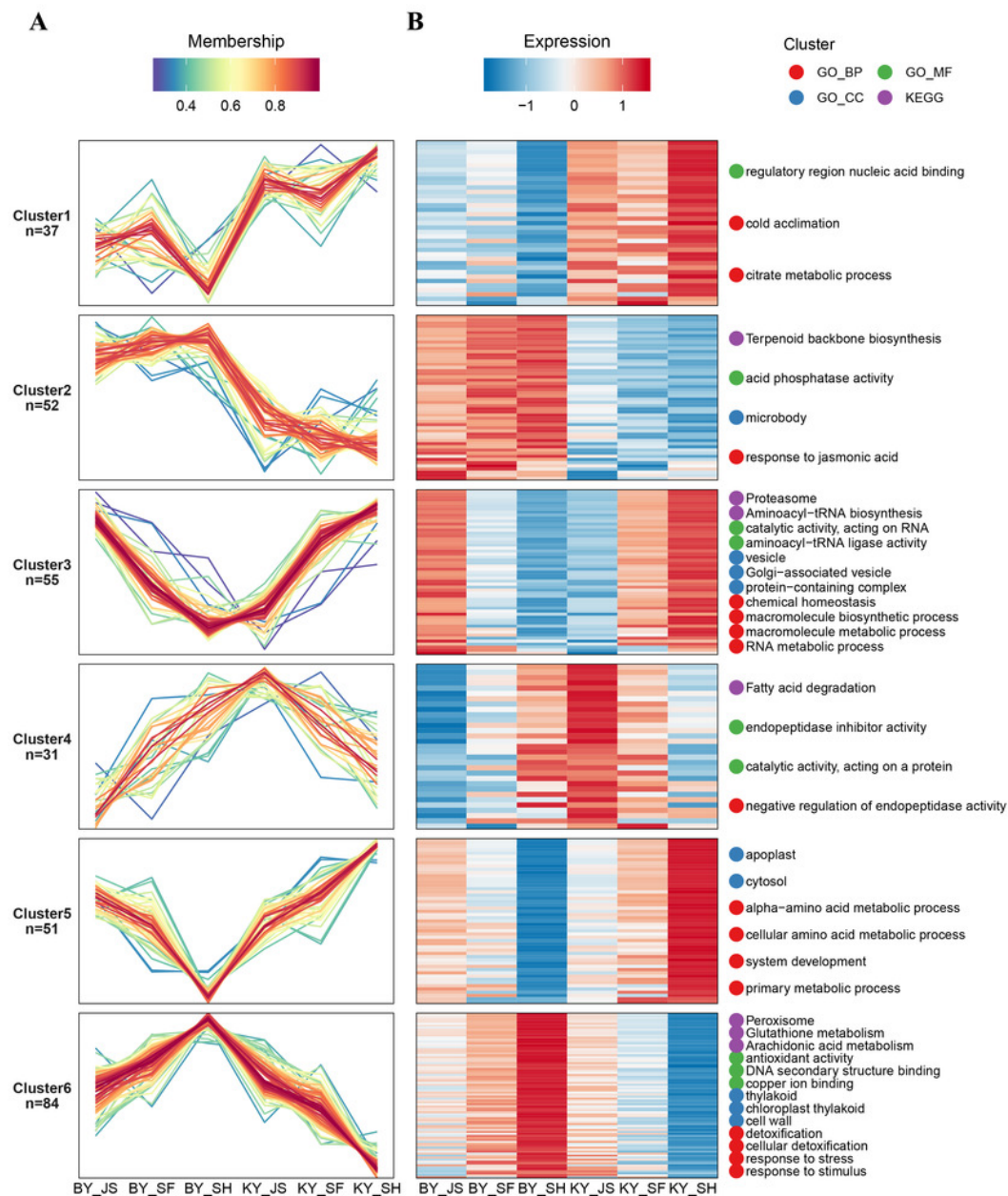
Figure 8

Clustering of differential abundance proteins.

A: DAPs identified in the anther development were divided into six clusters in BY_JS vs KY_JS, BY_SF vs KY_SF and BY_SH vs KY_SH. B: The expression patterns and different metabolic pathways of DAPs.
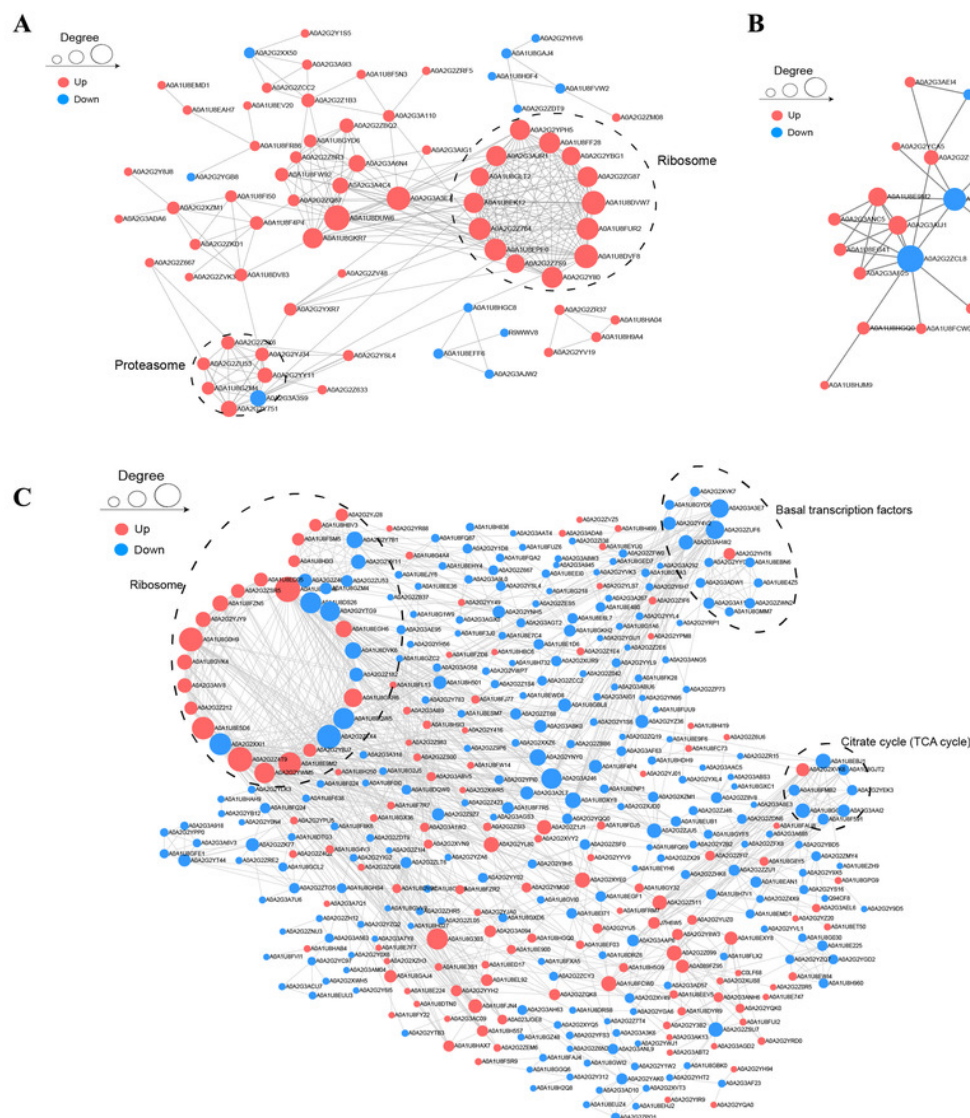
Figure 9

DAPs were quantified at meiosis, tetrad and binucleate stages by parallel reaction monitoring (PRM).

A: BY_JS vs. KY_JS. B: BY_SF vs. KY_SF. C: BY_SH vs. KY_SH.